

# Zero non-detection zone assessment for anti-islanding protection in rotating machines based distributed generation system

Ahmad G. Abd-Elkader | Saber M. Saleh

Electrical Engineering Department, Faculty of Engineering, Fayoum University, Fayoum, Egypt

## Correspondence

Saber M. Saleh, Electrical Engineering Department, Faculty of Engineering, Fayoum University, Fayoum, Egypt.  
 Email: [sabermssh@gmail.com](mailto:sabermssh@gmail.com)

## Summary

The challenges for a reliable operation of electrical power system have increased due to the presence of multi-distributed generation units (DGs) in the distribution systems in order to meet the increase of the load demand. Detection of unintentional islanding situation is very important as non-detection of islanding situation could result in a cascaded failure of the system. If the islanding situation remains undetected, the instability in the islanded part can lead to a complete failure of the electrical power system. This paper introduces a new passive scheme for islanding detection, which is suitable for multi-distributed generation units based on rotating machines. The proposed method is based on the measurements of the system voltage and frequency to compute two indices called the islanding index and harmonics index. The islanding index is the main index used to discriminate and identify the islanding situation. However, the harmonics index in conjunction with a strategy called speed reduction strategy assists the islanding index to discriminate between islanding situation in case of a close power match and system disturbances. The simulation studies were conducted in MATLAB/SIMULINK environment, and various cases have been considered, such as normal operation, islanding operation, sudden load change, DG tripping, separation of some DG units, faults, etc.

The novelty of the proposed strategy is that it provides fast detection and has **zero** nondetection zone compared with the existing detection methods. Moreover, the proposed strategy has no effect on the power quality, and the maximum detection time is almost **350** ms at a close power match. The results indicate that the proposed scheme is successful in discrimination of the islanding conditions from other grid disturbances, revealing its great potential to be able to detect islanding events. Finally, the proposed method is applied only for rotating machine based DGs, such as wind turbines. Wind farms'

**Abbreviations:** DG, Distributed Generation; NDZ, Non-Detection Zone; IDMs, Islanding Detection Methods; PDM, Passive Detection Methods; DFIG, Doubly-Fed Induction Generators; DFT, Discrete Fourier Transform;  $K_S$ , Islanding Index;  $K_C$ , Threshold Value of Islanding Index;  $K_H$ , Harmonics Index;  $K_{HO}$ , Threshold Value of Harmonics Index; SRS, Speed Reduction Strategy.

power generation system based on doubly-fed induction generators is introduced in this paper as an example of DGs units.

**KEYWORDS**

islanding detection, anti-islanding protection, non-detection zone, distributed generations

## 1 | INTRODUCTION

Distributed generation (DG) units are connected directly to the utility distribution network. If properly planned and operated, DG units may have the ability to interact with the utility grid, increase the flexibility, and improve the efficiency of the system. However, the integration of DG units into the utility distribution network is associated with some problems, such as power quality problems, protection coordination, and islanding operation.<sup>1,2</sup> One issue that should be considered is the islanding operation. Islanding operation is a situation in which the DG units continue to supply fully or partially the local loads after the grid is disconnected.<sup>1-8</sup> This situation can lead to many potential hazards since the DG units are without control and supervision of utility. Therefore, this situation should be detected and protected rapidly. Considering the serious consequences islanding situation can cause, IEC-62116, IEEE STD-1547, and IEEE STD-929 standards decided that islanding situation should be detected and prevented.<sup>1-3</sup> IEEE Standard 1547.4-2011 determines a delay of 2 seconds for islanding situation detection.<sup>9,10</sup>

This paper consists of seven sections as follows: Section 2 demonstrates the current detection methods and the study contributions. Section 3 shows the description of the test system under consideration. In Section 4, the proposed method's details are introduced. Section 5 discusses the results of the simulation and the proposed method's performance. Finally, Sections 6 and 7 present the discussion and conclusions, respectively.

## 2 | CURRENT ISLANDING DETECTION METHODS AND STUDY CONTRIBUTION

Several islanding detection methods (IDMs) have been developed and reported in the literature under different categories, discriminated as remote methods and local methods. The first category is based on the principle of communication among the utility grid and the DG units. Although this category is expensive and subject to communication failures, it has zero non-detection zone (NDZ). The NDZ is an interval where IDMs are unable to

identify the islanding situation on time.<sup>8</sup> Power line communication and supervisory control and data acquisition methods are the main remote detection methods.<sup>5</sup> The second category of detection schemes is further divided into passive and active schemes.<sup>3-7</sup>

### 2.1 | Active methods

Active detection methods detect islanding operation based on the response of the DG when small periodic disturbances are intentionally injected on the frequency or voltage of the power system<sup>4-7</sup> in order to force the frequency or the voltage to drift up or down during islanding situation.<sup>1</sup> Despite their high accuracy to discriminate islanding events with a very small NDZ, active methods have an adverse influence on the distribution system operation owing to injection disturbances.<sup>4-9</sup> Moreover, it requires a time to inject a disturbance to detect the voltage or frequency changes.<sup>19,33</sup> A complete survey of active methods can be found in the literature.<sup>2-9</sup>

### 2.2 | Passive Methods

This paper concentrates on passive islanding detection. Passive detection methods (PDM) depend on measuring one or more system parameters, such as voltage, frequency, voltage angle, etc, at the DG unit terminals and compare it with a specified threshold value to judge whether there is an islanding situation.<sup>5,22</sup> If the measurements exceed the threshold values, the islanding relay makes a decision to shut down the DG unit from the network.<sup>4-9</sup> A complete survey on the passive detection methods can be found in the literature.<sup>4-7</sup> Passive detection methods are preferred because they are simple, easy for implementation, and applied to any network structure.<sup>1</sup> Moreover, they do not have any effect on the system stability and power quality. However, the major drawbacks of PDM are the large NDZ compared to active methods and low discrimination between non-islanding and islanding conditions.<sup>9,23</sup>

Interestingly, new passive methods have been recently introduced. The proposed method in Ref. 19 uses the voltage index at the DG unit and the line current at

the main bus. Although the method has zero non-detection zone and can be used for multiple DG units, the authors considered only the lower limits of the voltage and frequency to determine the threshold. In Ref. 20, the authors present a passive method for both inverter and synchronous machine-based DG units. However, the proposed method has smaller NDZ. Another method based on the dynamic load behavior is presented in Ref. 1. The method has smaller NDZ and the threshold for islanding detection depends on the load type. Moreover, a new scheme based on total variation filtering for a modal voltage signal is proposed in Ref. 32. The proposed scheme is found to be working effectively but the threshold selection is based on simulation results.

Recently, some computational intelligent methods in combination with modern signal processing techniques have been introduced to get rapid detection of islanding condition, such as artificial neural network,<sup>11-16,27-31</sup> fuzzy logic,<sup>15-18,28</sup> and wavelet.<sup>15-17,24-28</sup> In spite of the outstanding features and the capability of these intelligent methods to determine the most proper combination of features, as well as thresholds, that can reduce the NDZ, such intelligent methods need additional software and hardware support and are difficult to implement in practice.<sup>1,19</sup> In addition, intelligent methods need higher execution time due to the high level of complexity. Furthermore, their performance is also governed by appropriate data updates and the impact of system reconfiguration.<sup>3,19</sup>

### 2.3 | The objective and contributions of this article

In spite of many research of islanding algorithms in this area, more islanding schemes are still needed. The main objective of this paper is to propose an accurate scheme for islanding detection in the distribution networks with multiple DG units based on rotational energy conversion. The proposed algorithm uses the system voltage and frequency to compute two indices called the islanding index and harmonics index. These indices are used in conjunction with an assistant strategy called speed reduction strategy to detect islanding condition. The main contributions of this paper are as follows:

- The suggestion of a simple practical islanding scheme for DGs based on rotating machines.
- Accurate discrimination between islanding and non-islanding events, without any effects on the system stability or the power quality.
- The proposed scheme is straightforward, easy to implement in practice, and has zero NDZ.

## 3 | MODEL DESCRIPTION

The proposed method is implemented on the distribution network shown in Figure 1. The distribution network is composed of four DG units (each one 5 MW, 1 MVAR) connected to a 20 kV distribution network. Each DG unit (wind farm) operates at 575 V and connected to 20 kV distribution network by a step-up transformer (5 MVA, 60 Hz, 575 V/20 kV). Moreover, the utility is connected to the distribution networks by a step-down transformer (50 MVA, 60 Hz, 120/20 kV). The DG units use doubly-fed induction generators (DFIG). The stator is connected directly to the network while the rotor is connected to the network through an AC/DC/AC IGBT-based PWM converter. The test system is modeled using Matlab/Simulink. The system parameters are mentioned in Table.1.

## 4 | THE PROPOSED ISLANDING DETECTION STRATEGY

Generally, the PDMs suffer from an inherent disadvantage of large non-detection zone. Moreover, PDMs require accurate thresholds for the system parameters. In the presence of DG units, the exact detection of islanding

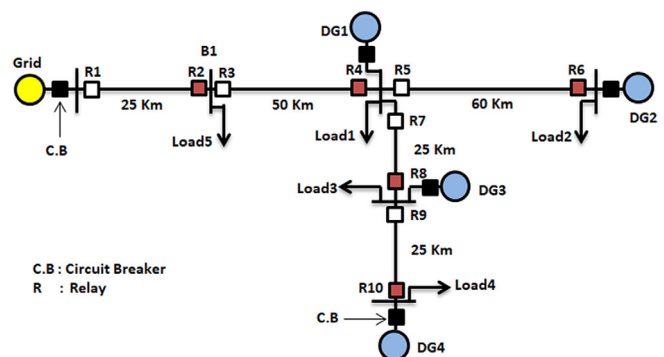


FIGURE 1 Model of the power system under study [Colour figure can be viewed at wileyonlinelibrary.com]

TABLE 1 The power system parameters

<b>Grid</b>	<b>2500 MVA;120 kV; 60 Hz.</b>
Grid transformer	Step down; 50 MVA; (120/20) kV
DG unit	5 MW;1MVAR; 575 V; 60 Hz.
DG transformer	Step up; 10 MVA; (575/20) kV
Transmission line parameters	R1 = 0.1153 Ω/km; R0 = 0.413 Ω/km; X1 = 1.05 mH/km; X0 = 3.32 mH/km; C1 = 11.33 nF/km; C0 = 5.01 nF/km;
R4, R6, R8, R10	Islanding detection relays at DG units

operation becomes difficult due to the complexity of observing the system parameters. The main target of this paper is to improve the performance of PDMs and eliminate the NDZ for DG units based on rotational energy conversion. This study introduces a passive detection scheme for multi-distributed generation units. The proposed scheme is based on a new index, entitled the islanding index, to detect the islanding event of DG units. Moreover, a band of harmonics is utilized as a further index called harmonics index to assist the detection of the islanding condition at a close power match. The strategy starts with voltage and frequency measurements at the DG site, and then Fourier analysis is used to extract the fundamental voltage signal and its harmonics in order to calculate the islanding index and harmonics index as follows:

#### 4.1 | Fourier analysis (discrete Fourier transform)

The analysis of this strategy starts with extracting the fundamental voltage signal and its harmonics at each DG unit. A Fourier analysis over a sliding window of one cycle of the fundamental frequency (60 Hz) is first applied to the measured voltage signals at the DG unit. It computes the phase voltages,  $V_a$ ,  $V_b$ , and  $V_c$ , at a specified frequency as follows.

Let  $v(m)$  be a discrete-time periodic voltage signal measured at the target DG unit. Let  $M$  samples be denoted as  $v(0), v(1), v(2), v(m) \dots v(M-1)$ . The discrete Fourier transform (DFT) of the discrete voltage signal  $v(m)$  is denoted by  $V(h)$  and given by,

$$V(h) = \sum_{m=0}^{M-1} v(m) e^{-j2\pi hm/M} \quad (1)$$

where  $h = 0, 1, 2 \dots M-1$ . We can get the discrete form of the voltage signal  $v(m)$  from its DFT by using inverse discrete Fourier transform (IDFT) as follows.

$$v(m) = \frac{1}{M} \sum_{h=0}^{M-1} V(h) e^{j2\pi hm/M} \quad (2)$$

Now, we can write the DFT equation as follows:

$$V(h) = \sum_{m=0}^{M-1} v(m) U_M^{mh} \quad (3)$$

where  $U_M = e^{j2\pi/M}$

Now, the equation of DFT could be evaluated for the fundamental frequency and harmonics ( $h = 0, 1, 2, \dots, M-1$ ). For  $M$ -point voltage vector,  $v_M$  and  $M \times M$  matrix  $U_M$ , the DFT equation can be written in the matrix form as follows:

$$V_M = U_M v_M$$

$$\begin{bmatrix} V(0) \\ V(1) \\ V(2) \\ \vdots \\ \vdots \\ V(M-1) \end{bmatrix} = \begin{bmatrix} 1 & 1 & 1 & \dots & 1 \\ 1 & U_M & U_M^2 & \dots & U_M^{M-1} \\ 1 & U_M^2 & U_M^4 & \dots & U_M^{2(M-1)} \\ \vdots & \vdots & \vdots & \dots & \vdots \\ \vdots & \vdots & \vdots & \dots & \vdots \\ 1 & U_M^{M(M-1)} & U_M^{2(M-1)} & \dots & U_M^{(M-1)(M-1)} \end{bmatrix} \begin{bmatrix} v(0) \\ v(1) \\ v(2) \\ \vdots \\ \vdots \\ v(M-1) \end{bmatrix} \quad (4)$$

IDFT may be written in the matrix form as follows:

$$v_M = U_M^{-1} V_M \quad (5)$$

where  $U_M^{-1} = \frac{1}{M} U_M^*$

$U_M^*$  is the complex conjugate of  $U_M$ .

#### 4.2 | The islanding index $K_S$

The proposed islanding index mainly depends on the variations in the system frequency and the fundamental voltage signal. Now, we can evaluate the phase voltages,  $V_a, V_b$ , and  $V_c$ , for the fundamental frequency (at  $h = 1$ ). Then the positive sequence component,  $V_s$ , of the voltage (60 Hz) is obtained as follows:

$$V_s = (V_a + aV_b + a^2V_c)/3 \text{ where } a = 1 \angle 120^\circ \quad (6)$$

In the next step, the frequency ( $f$ ) is measured at the target DG unit, and then the islanding index is calculated. The islanding index  $K_S$  is defined by Equation (7) as a function of the voltage and frequency variations as follows.

$$K_S = \left[ (\Delta V)^{K_m - \Delta f} - 1 \right] \quad (7)$$

where  $\Delta V$  and  $\Delta f$  represent the changes in the system voltage (in per-unit) and frequency, respectively, and  $K_m$  is a constant, which relies on the measured frequency. These changes in the system voltage and frequency are given by the following equations:

$$\Delta V = |V_s - V_b| \text{ in pu} \quad (8)$$

$$\Delta f = |f_s - f_b| \text{ in Hz} \quad (9)$$

where  $V_b$  and  $V_s$  are the base voltage and measured voltage of the system, respectively. Moreover,  $f_b$  and  $f_s$  are the base frequency and measured frequency of the system, respectively.  $K_m$  is a constant, which has two values deduced as follows:

According to IEEE standard-1547-2011, the system frequency should be between 59.3 and 60.5 Hz. According to those limits, the upper difference is 0.5 Hz (60.5-60) and the lower difference is 0.7 Hz (60-59.3). Therefore, in order to have one threshold corresponding to the upper and lower differences of the frequency, the constant,  $K_m$ , should have two values; first,  $K_m$  equals 0.5 when the measured frequency,  $f_s$ , is higher than 60 Hz. Second,  $K_m$  equals 0.7 when the measured frequency,  $f_s$ , is lower than 60 Hz.

### 4.3 | The threshold value $K_o$ of the islanding index

As mentioned earlier according to IEEE standard-1547-2011, the system voltage should be between 0.88 and 1.10 pu. Moreover, the system frequency should be between 59.3 and 60.5 Hz. In this study, the base voltage,  $V_b$ , is 1 pu and the base frequency,  $f_b$ , is 60 Hz. Now, we can easily calculate the threshold value,  $K_o$ , for islanding detection from the definition of  $K_S$  given by Equation (7).

a) Consider the lower limits of the voltage and frequency (0.88 pu and 59.3 Hz). According to Equation (7);

$$\Delta f = |f_{s \text{ low}} - f_b| = |59.3 - 60| = 0.7 \text{ and } k_m = 0.7$$

$$\Delta V = |V_{s \text{ low}} - V_b| = |0.88 - 1| = 0.12 \text{ pu}$$

Using the previous data, we get  $K_o = [(\Delta V)^{K_m - \Delta f} - 1] = [(0.12)^{0.7 - 0.7} - 1] = 0$

Consider the upper limits of the voltage and frequency (1.10 pu and 60.5 Hz). According to Equation (7);

$$\Delta f = |f_{s \text{ high}} - f_b| = |60.5 - 60| = 0.5 \text{ and } k_m = 0.5$$

$$\Delta V = |V_{s \text{ high}} - V_b| = |1.10 - 1| = 0.10 \text{ pu}$$

Using the previous data, we get  $K_o = [(\Delta V)^{K_m - \Delta f} - 1] = [(0.10)^{0.5 - 0.5} - 1] = 0$ .

We can make two important observations here. First, the threshold value,  $K_o$ , has the same value (zero) at the

upper and lower limits of the system voltage and frequency. Second, the situation is defined as an islanding operation if the islanding index,  $K_S$ , has a positive value as follows.

During normal operation and system disturbances, the voltage and frequency are within the allowed limits. Therefore, the difference ( $K_m - \Delta f$ ) will be positive and the factor  $(\Delta V)^{K_m - \Delta f}$  will be always less than 1. Consequently, the islanding index,  $K_S$ , will be always less than zero (negative).

However, during islanding operation, the voltage and frequency are outside the allowed limits. Therefore, the difference ( $K_m - \Delta f$ ) will be negative, and the factor  $(\Delta V)^{K_m - \Delta f}$  will be always higher than 1. Consequently, the islanding index,  $K_S$ , will be always greater than zero (positive).

To aid the indication of the threshold value,  $K_o$ , for islanding detection from the definition of  $K_S$ , we show the islanding index vs the frequency plot in Figure 2 at the upper and lower limits of the voltage changes (0.10 and 0.12 pu respectively).

### 4.4 | The harmonics index $K_h$

The grid islanding switching effect and distributed generation units, which considered a source of harmonics with a noticeable value of harmonics that depends upon the generator design and its power electronics technology, produce distorted voltage. The harmonic distortions in voltage waveform are negligible in the grid-connected mode of operation since the utility grid acts as a strong voltage source. During islanding operation, the voltage harmonics vary considerably owing to the current harmonics produced by the power electronics converters and the grid switching.

During the Fourier analysis (DFT) of the distorted voltage signal in case of islanding operation, a set of harmonics is observed and depends fully on the case study system. This set is all harmonics starting at the second harmonic and ending at the eighth harmonic. Summation of the magnitudes of those harmonics is defined as the harmonics index,  $K_h$ , and is given by the following equation.

$$K_h = \sum_{h=2}^8 V(h) \quad (10)$$

Table 2 shows the percentages of those harmonics relative to the fundamental component of the voltage during normal operation and islanding at a small power mismatch.

As shown in Table 2, the harmonics index,  $K_{ho}$ , during islanding at a small power mismatch is higher than

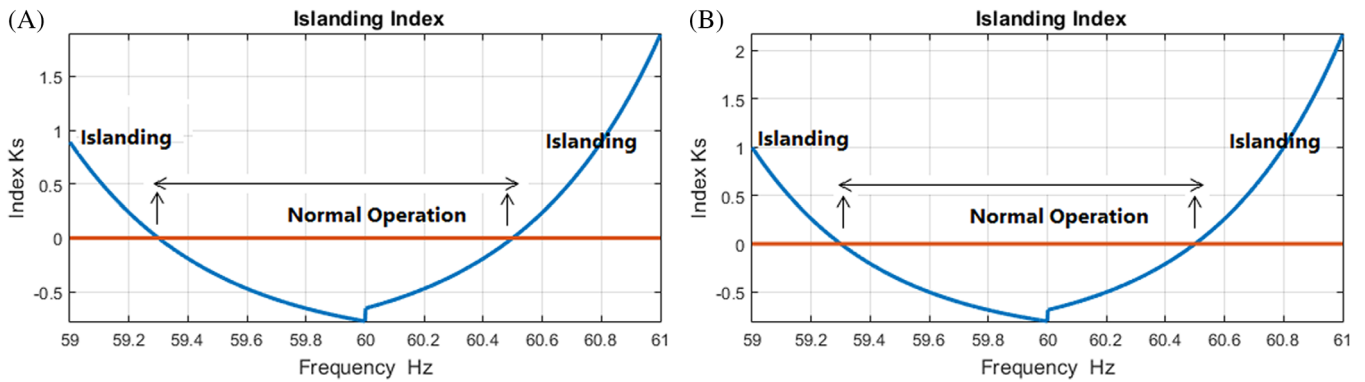


**FIGURE 2** Islanding index at the upper and lower limits of the voltage. (A)  $\Delta V = 0.10$  pu (B)  $\Delta V = 0.12$  pu [Colour figure can be viewed at wileyonlinelibrary.com]

**TABLE 2** The percentages of harmonics relative to the fundamental

Harmonic order	Percentage at Islanding at small power mismatch	Percentage at Normal operation
2nd harmonic (120 Hz)	1.74	0.10
3rd harmonic (180 Hz)	0.47	0.09
4th harmonic (240 Hz)	0.43	0.09
5th harmonic (300 Hz)	0.53	0.01
6th harmonic (360 Hz)	0.37	0.12
7th harmonic (420 Hz)	0.35	0.07
8th harmonic (480 Hz)	0.25	0.10
Total percentage	4.14	0.58

the harmonics index during normal operation. Consequently, the threshold of the harmonics index,  $K_{ho}$ , should be less than or equal to 4.14% (relative to the fundamental component) to include islanding situation at a small power mismatch. Therefore, in this study, the threshold of the harmonics index,  $K_{ho}$ , is set to 4% as a safety margin for stability and is given as follows:

$$K_{ho} = 4\% \times V_{Ph}(\text{fundamental}) = 4\% \times 11547 = 462 \text{ V} \quad (11)$$

The harmonics index,  $K_h$ , is used as an assistant index to the islanding index only in the case of islanding operation at a close power match.

### 4.5 | The proposed islanding detection method

The proposed method starts with measuring the phase voltages and frequency at each DG unit in the network,

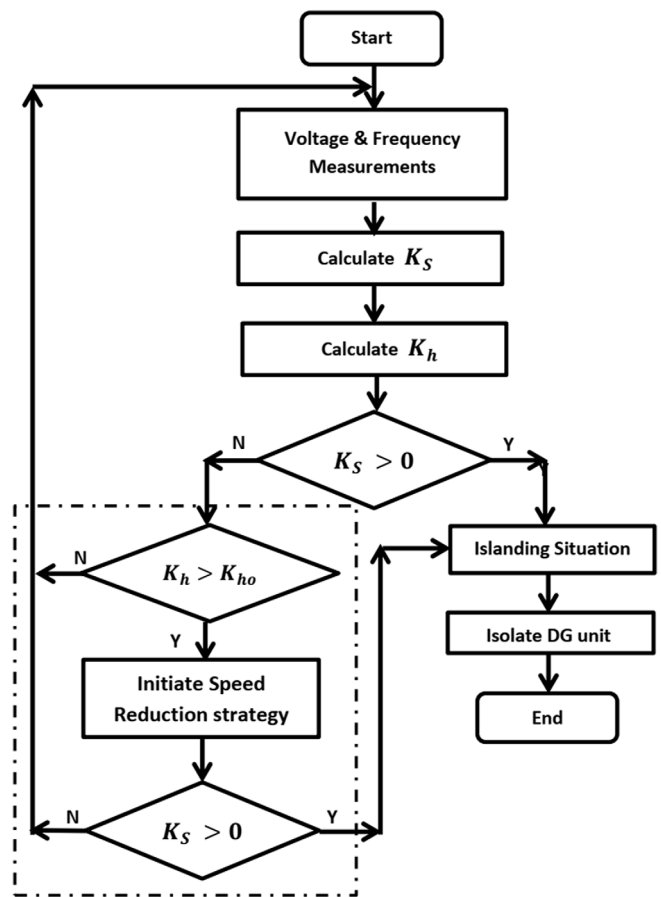


**FIGURE 3** Flowchart of the proposed algorithm

and then the islanding index,  $K_s$ , and the harmonics index,  $K_h$ , are calculated as mentioned earlier. The proposed islanding detection method follows the flowchart illustrated in Figure 3. The following sections explain the proposed strategy through the different situations of islanding condition.

#### 4.5.1 | Islanding at a large power mismatch

In this case, the islanding situation is detected when the islanding index,  $K_s$ , has only a positive value as illustrated in Figure 2.

#### 4.5.2 | Islanding at a close power match

In this case, the islanding index,  $K_s$ , has a negative value and islanding situation detection is impossible. This problem is fixed by utilizing the harmonics index. When islanding condition happens, the current harmonics generated by the inverters are transmitted to the loads, which generate voltage harmonics that can be measured. The variation of harmonics index beyond a certain threshold can be used to initiate a strategy called speed reduction strategy (SRS). SRS reduces the speed of DFIG by 5% in order to change the output power of the DG units for a certain time (300 ms). The purpose behind SRS is to transform the islanding situation from a close power match to a large power mismatch. This action leads to a remarkable variation in the islanding index,  $K_s$ , and becomes positive because of the loss of the utility grid. The islanding relays at the DG units detect those variations and trip the DG units. The dotted part in the flowchart indicates this case.

#### 4.5.3 | Separation of some DG units from the network

In the case of one or more DG units isolated from the rest of the system and continue providing the loads in the islanded portion, in such situation, the islanding is detected with the same way mentioned earlier in the previous sections.

#### 4.5.4 | Sudden load changes

During sudden load changes, the islanding index has a negative value, but the harmonics index variations may exceed the threshold. In such situation, a case of islanding condition is suspected and the islanding relay at the DG bus is alerted for an impending islanding situation. The islanding relay initiates the SRS and the islanding index,  $K_s$ , is monitored. If the islanding index,  $K_s$ , has a positive value, the condition will be defined as an islanding condition; otherwise, the condition will be defined as sudden load changes (normal operation).

## 5 | THE PROPOSED STRATEGY PERFORMANCE

The multiple DG system shown in Figure 1 is simulated for different conditions to demonstrate the proposed strategy performance. The detailed simulation studies have been conducted with MATLAB/SIMULINK software and various cases have been considered: normal operation, islanding operation, sudden load switching, transient voltage dip, DG unit switching, capacitor switching, asymmetrical faults, etc. During all simulations, the circuit breaker of the utility grid opens at  $t = 0.6$  second, which creates an islanding condition. The following sections explain the cases under consideration.

### 5.1 | Islanding condition at a large power mismatching

When the DG units operate in a grid-connected mode (normal operation), the system parameters are maintained by the utility grid. However, when the utility grid is disconnected, the support of the distribution network is lost. Thus, the system parameters are affected and the islanding index,  $K_s$ , is changed considerably. Simulation results presented in Figure 4 show the islanding index during normal and islanding conditions for the system described in Section 3. It can be seen from Figure 4 that once the islanding condition happens at  $t = 0.6$  second, the islanding index increases significantly and becomes greater than zero at each DG unit. The detection time of the islanding condition at each islanding relay is almost 150 ms. The proposed scheme can easily and rapidly detect the islanding condition with large power mismatches. During simulation, the total load demand is 16 MW and 2 MVAR, and for the DG system it is 20 MW and 5 MVAR. The power mismatch is 4 MW and 3 MVAR during this case.

### 5.2 | Islanding condition at a close power matching (zero power mismatch)

In this scenario, the support of the distribution network is lost and the system voltage and frequency are still within the allowed limits as shown in Figure 5. Therefore, no significant changes are detected in the islanding index,  $K_s$ , as indicated in Figure 6. However, considerable changes are detected in the harmonics index,  $K_h$ , due to loss of the grid as indicated in Figure 7. These variations are used to initiate the SRS at each DG unit according to the flowchart, and the islanding index is observed. The simulation results of Figure 8 show that

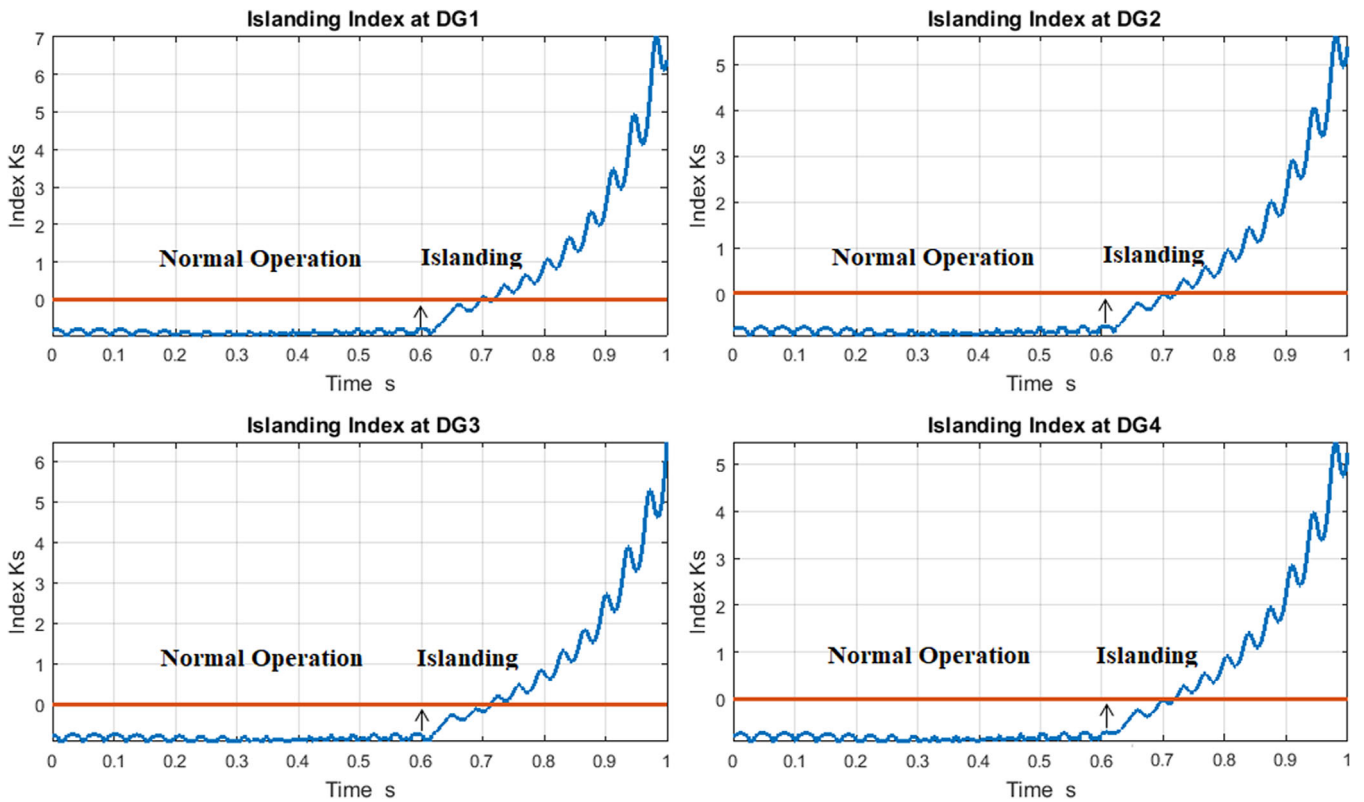


**FIGURE 4** Islanding index at DG units during islanding condition at a large power mismatch [Colour figure can be viewed at [wileyonlinelibrary.com](http://wileyonlinelibrary.com)]

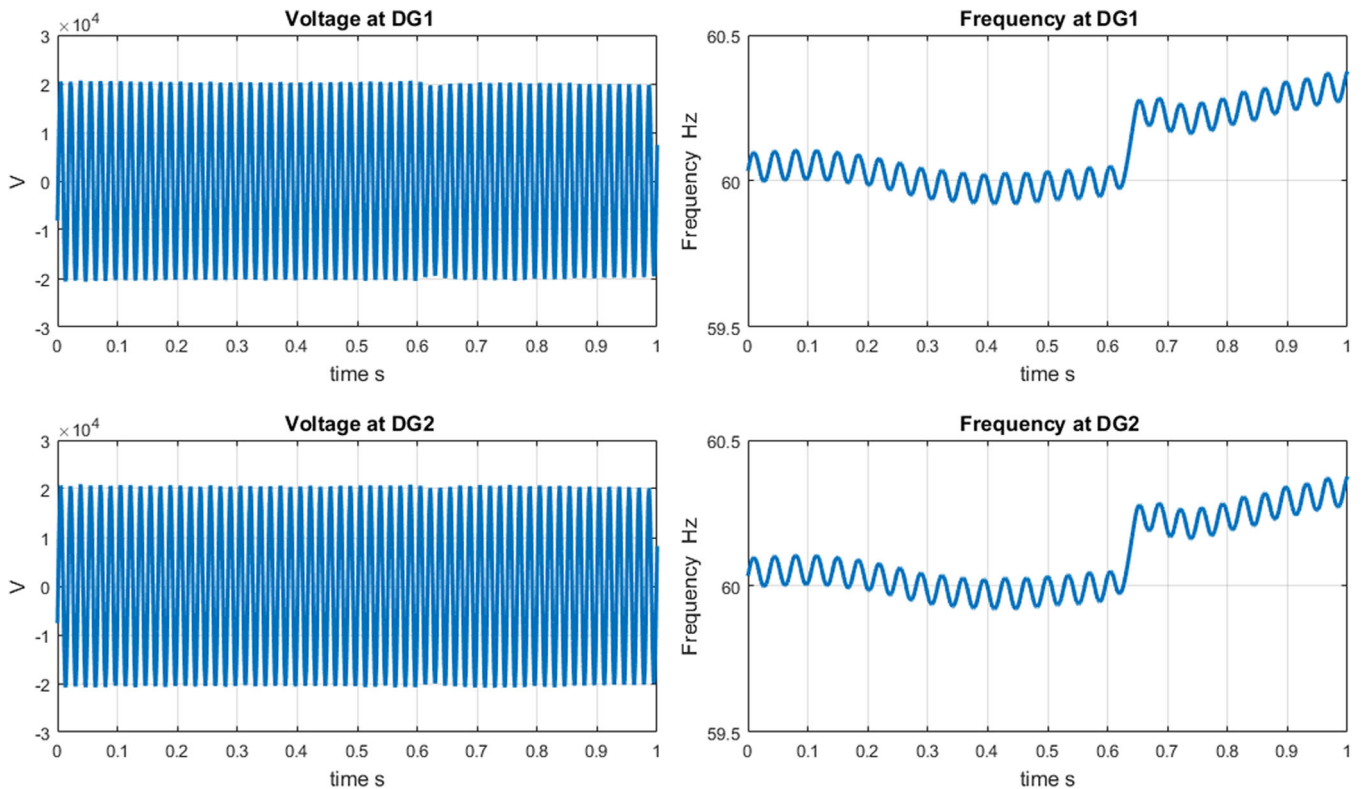


**FIGURE 5** Phase voltage and frequency at DG units (1 and 2) during islanding at zero power mismatch [Colour figure can be viewed at [wileyonlinelibrary.com](http://wileyonlinelibrary.com)]

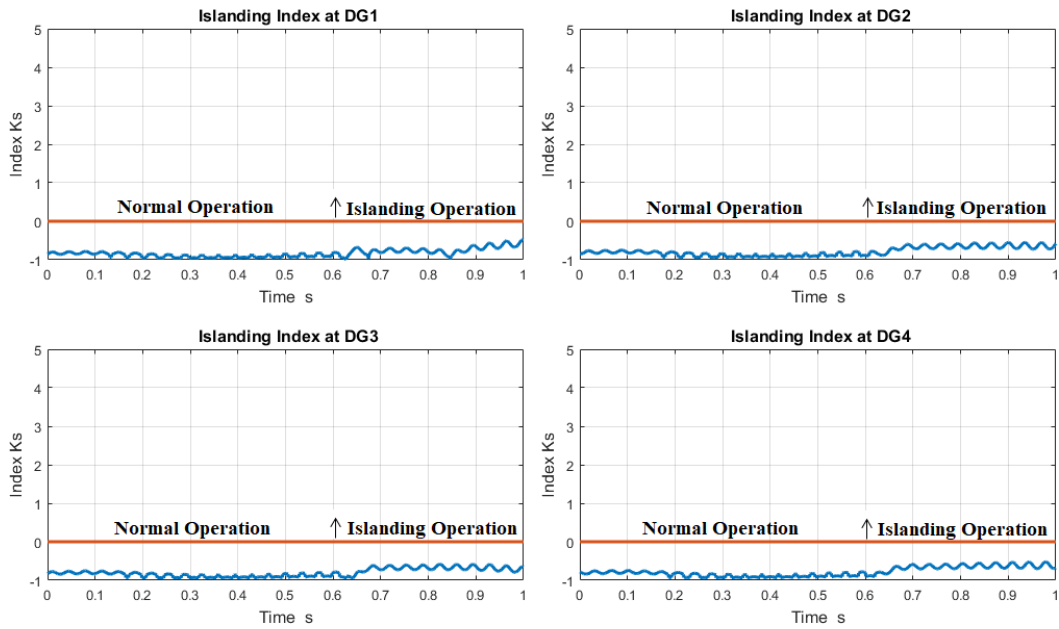


**FIGURE 6** Islanding index at DG units during normal operation and islanding at zero power mismatch **without** initiating SRS [Colour figure can be viewed at wileyonlinelibrary.com]

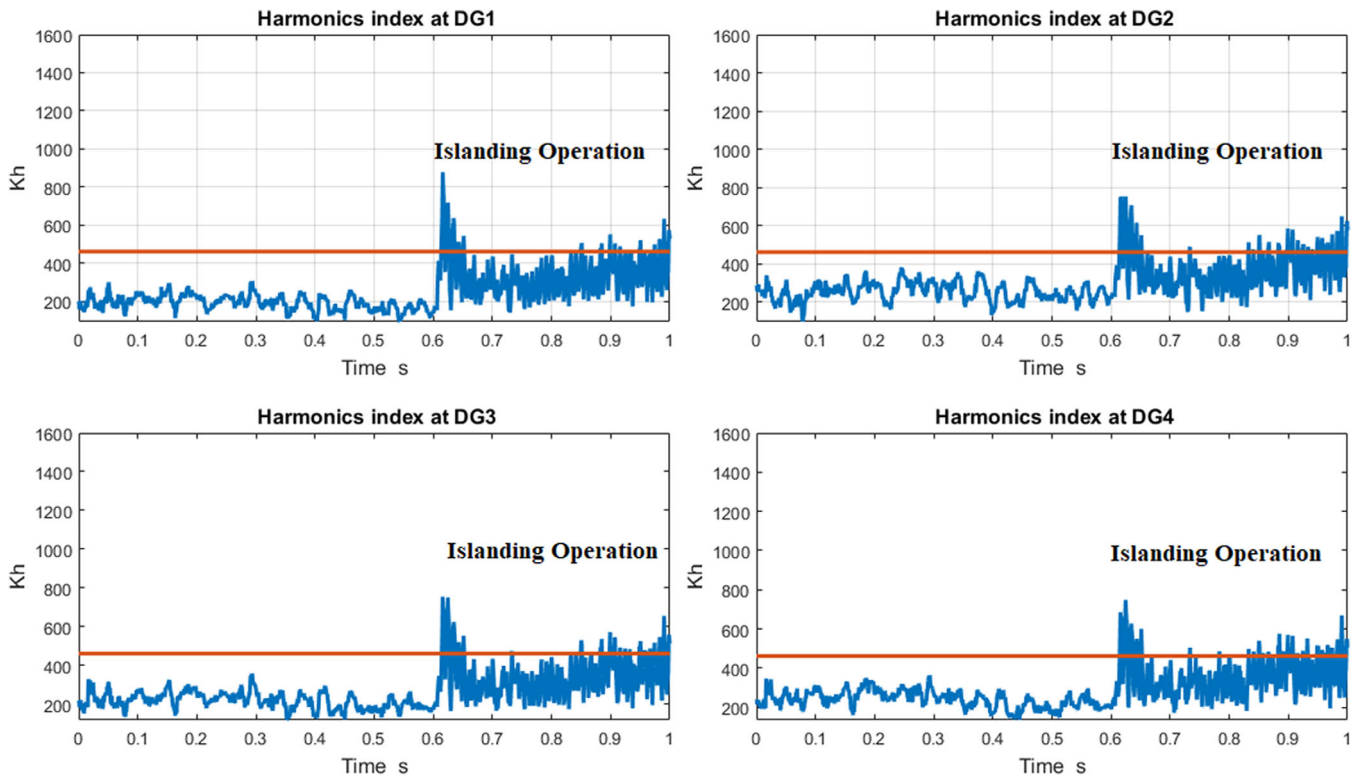


**FIGURE 7** Harmonics index  $K_h$  at DG units during normal operation and islanding at zero power mismatch **without** initiating SRS [Colour figure can be viewed at wileyonlinelibrary.com]

once SRS is initiated at  $t = 0.65$  second, the islanding index increases significantly and exceeds the threshold at each DG unit. The detection time in this case at each

relay is almost 350 ms. The total load demand during simulation is 20 MW and 5 MVAR and the power mismatch is zero.

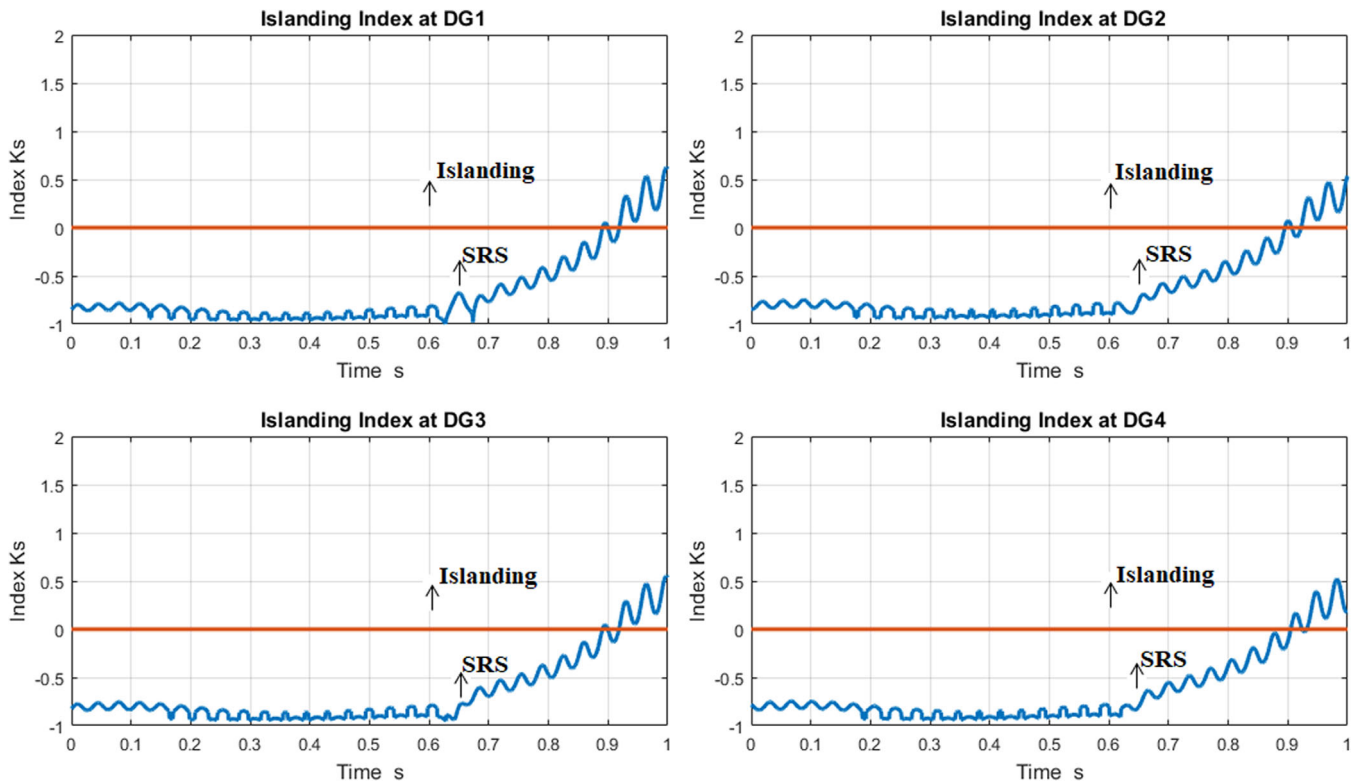


**FIGURE 8** Islanding index at DG units during normal operation and islanding at zero power mismatch with initiating SRS [Colour figure can be viewed at [wileyonlinelibrary.com](http://wileyonlinelibrary.com)]

### 5.3 | Sudden load change

In this case, the response of the proposed method will be further investigated for a sudden load change. The proposed method is tested by simulating the test system under a large load connection. A load increment of 4 MW and 1 MVAR is simulated at  $t = 0.15$  second at bus B1, when the total load is 16 MW and 4 MVAR. Simulation results of Figure 9 show that no significant changes are observed in the islanding index with regard to load increment at  $t = 0.15$  second. However, considerable changes are detected in the harmonics index,  $K_h$ , due to the sudden load change as indicated in Figure 10. These variations initiate the SRS at each DG unit, and the islanding index is monitored. The simulation results of Figure 9 indicate that no significant changes are also observed in the islanding index after SRS is initiated at  $t = 0.2$  second. In general, such sudden changes have no effects on the proposed method. Another islanding event at a close power match is also simulated at  $t = 0.6$  second and SRS is initiated at  $t = 0.65$  second as illustrated in Figure 9 in order to show the effect of SRS and discriminates between the two cases.

### 5.4 | Voltage dip and voltage rise

In this case, the proposed method response in non-islanding circumstances is also tested for power quality disturbances. Voltage dip (V. D) and voltage rise (V. R) are power quality disturbances that lead to a change in voltage of the system. During the simulation, the voltage is reduced to 90% of its rated value from 0.2 to 0.4 seconds and then increased to its rated value. It is clear from Figure 10 that when such disturbances occur (from 0.2 to 0.4 second), small variations are detected in the islanding index and still below the threshold. Moreover, an islanding condition is simulated at  $t = 0.6$  second as illustrated in Figure 11 in order to discriminate between the cases. The simulation results show that the proposed method discriminates the power quality disturbances from the islanding events.

### 5.5 | Islanding condition due to isolation of DG units from the network

In this scenario, two DG units (3 and 4) are islanded and continue feeding the local loads (L3 and L4) in the

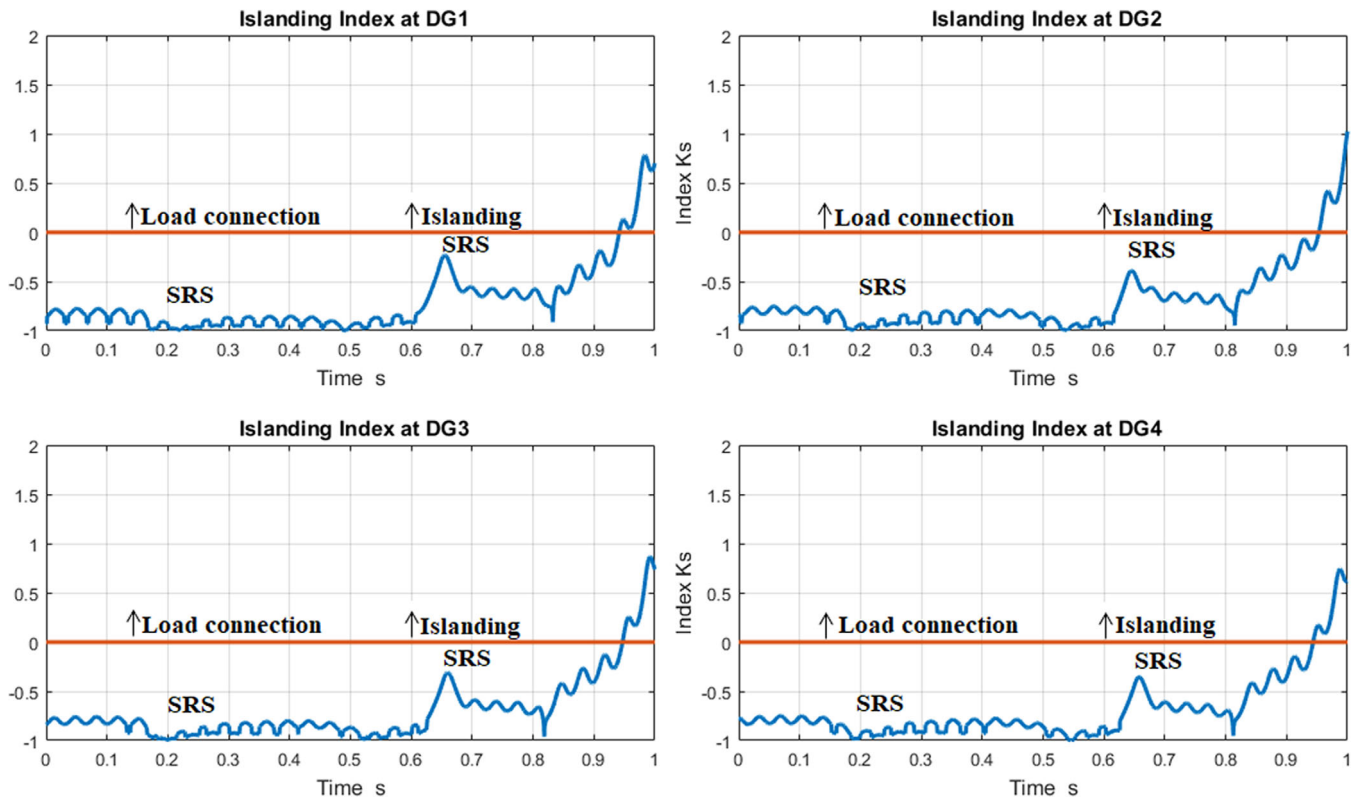


**FIGURE 9** Islanding index at DG units during load connection (at 0.15 second) and islanding at zero power mismatch (at 0.6 second) [Colour figure can be viewed at wileyonlinelibrary.com]

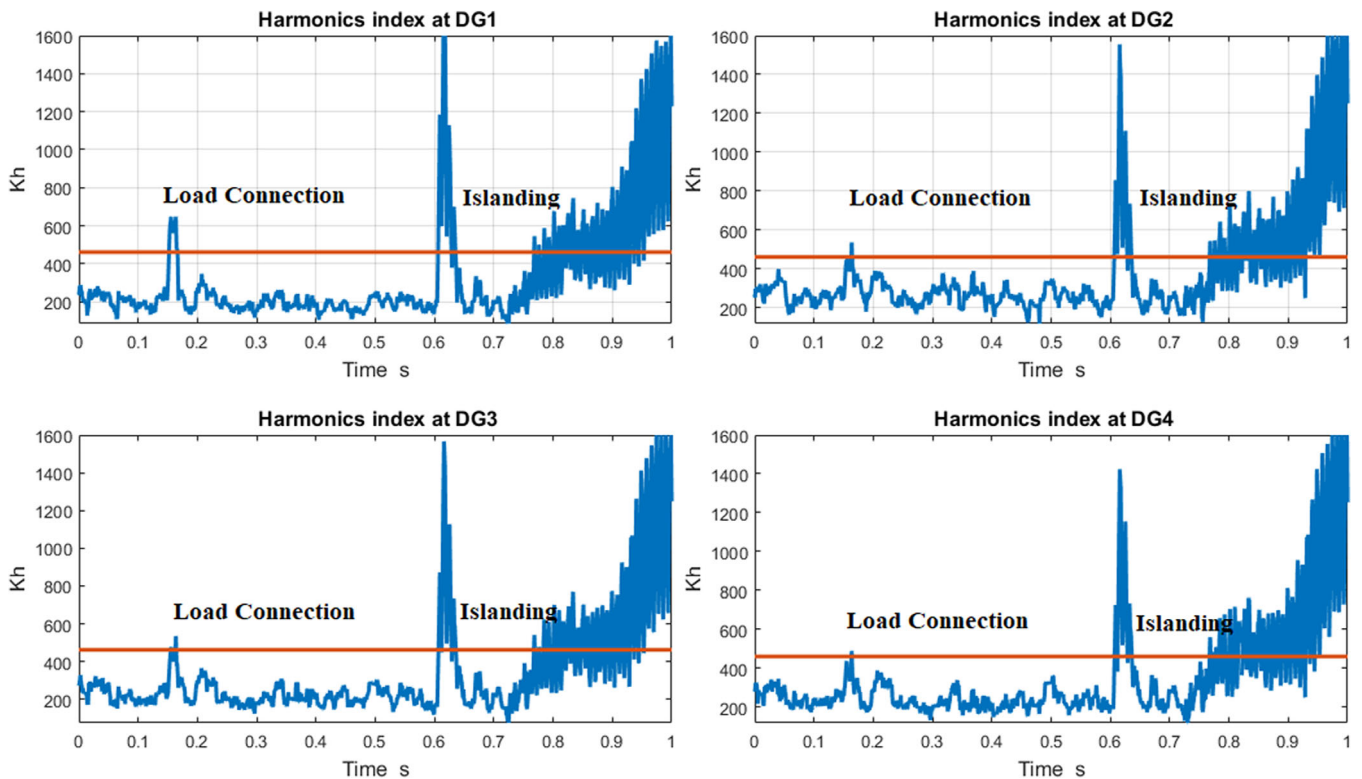


**FIGURE 10** Harmonics index  $K_h$  at DG units during load connection and islanding at zero power mismatch [Colour figure can be viewed at wileyonlinelibrary.com]

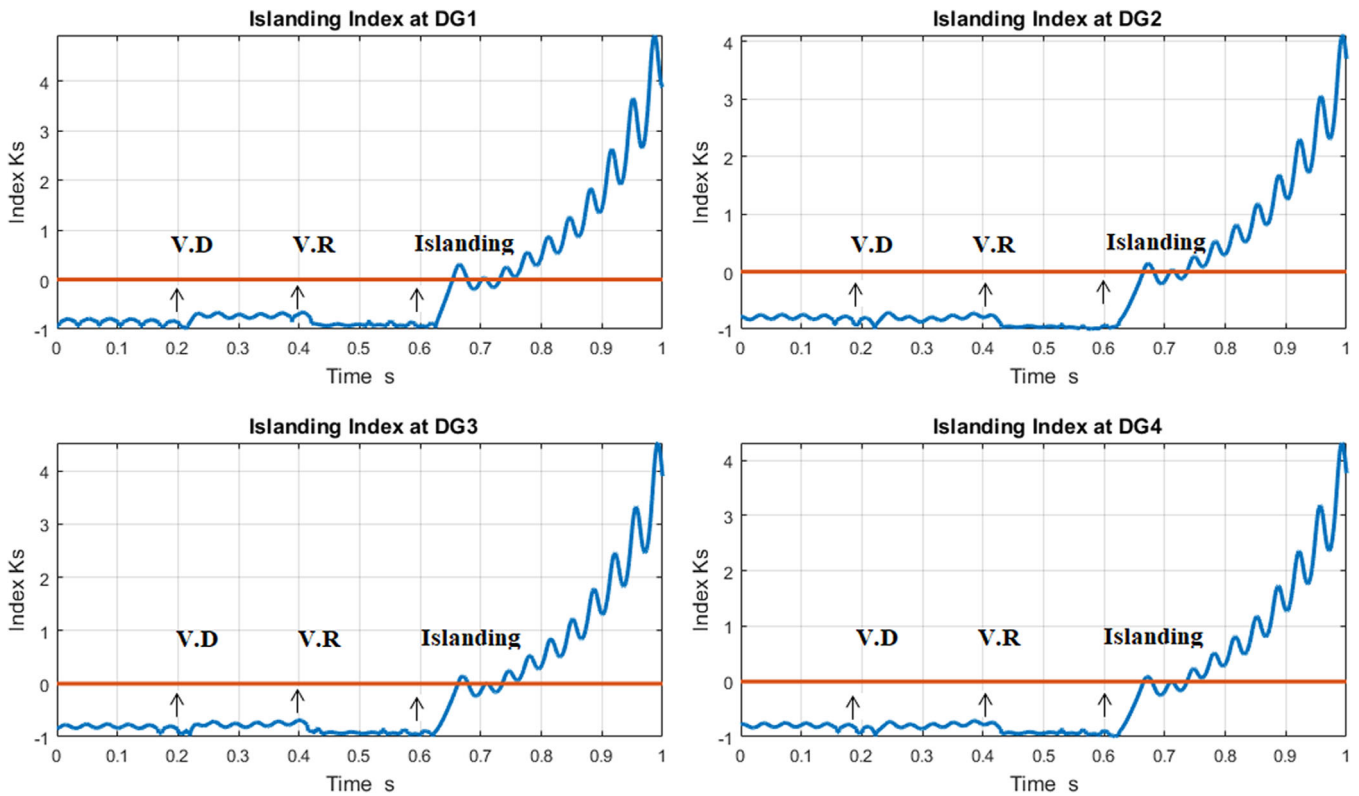


**FIGURE 11** Islanding index at DG units during Voltage sag, Voltage rise, and an islanding [Colour figure can be viewed at wileyonlinelibrary.com]

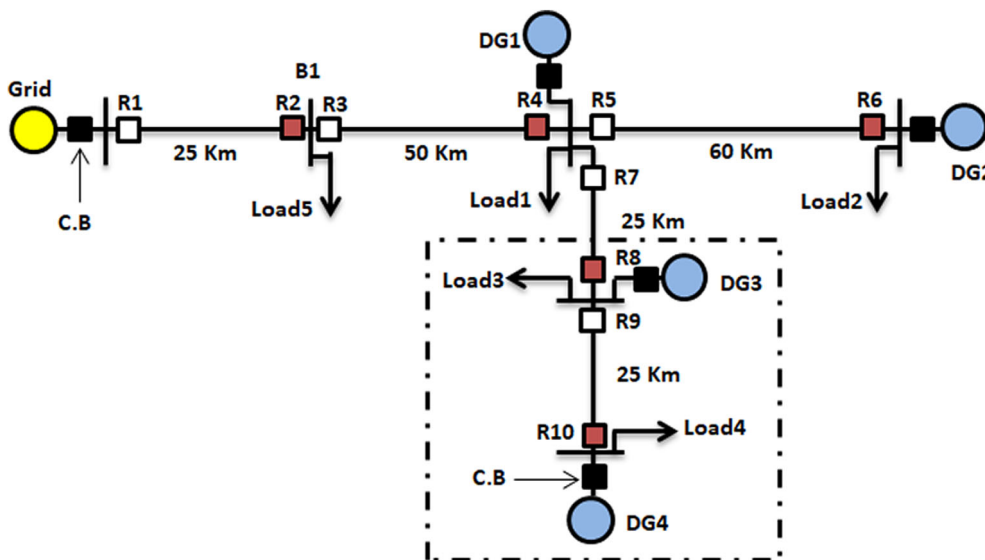


**FIGURE 12** Isolation of DG units (3 and 4) and the loads (L4 and L5) from the network [Colour figure can be viewed at wileyonlinelibrary.com]

islanded region while the other DG units (1 and 2) are still connected to the utility grid as shown in Figure 12. This islanding situation is simulated by disconnecting the transmission line (R7-R8) which isolates DG units

3 and 4 (10 MW and 2 MVAR) and the local loads L3 and L4 (8 MW and 2 MVAR) from the rest of the network (the part inside the dotted rectangle in Figure 12).

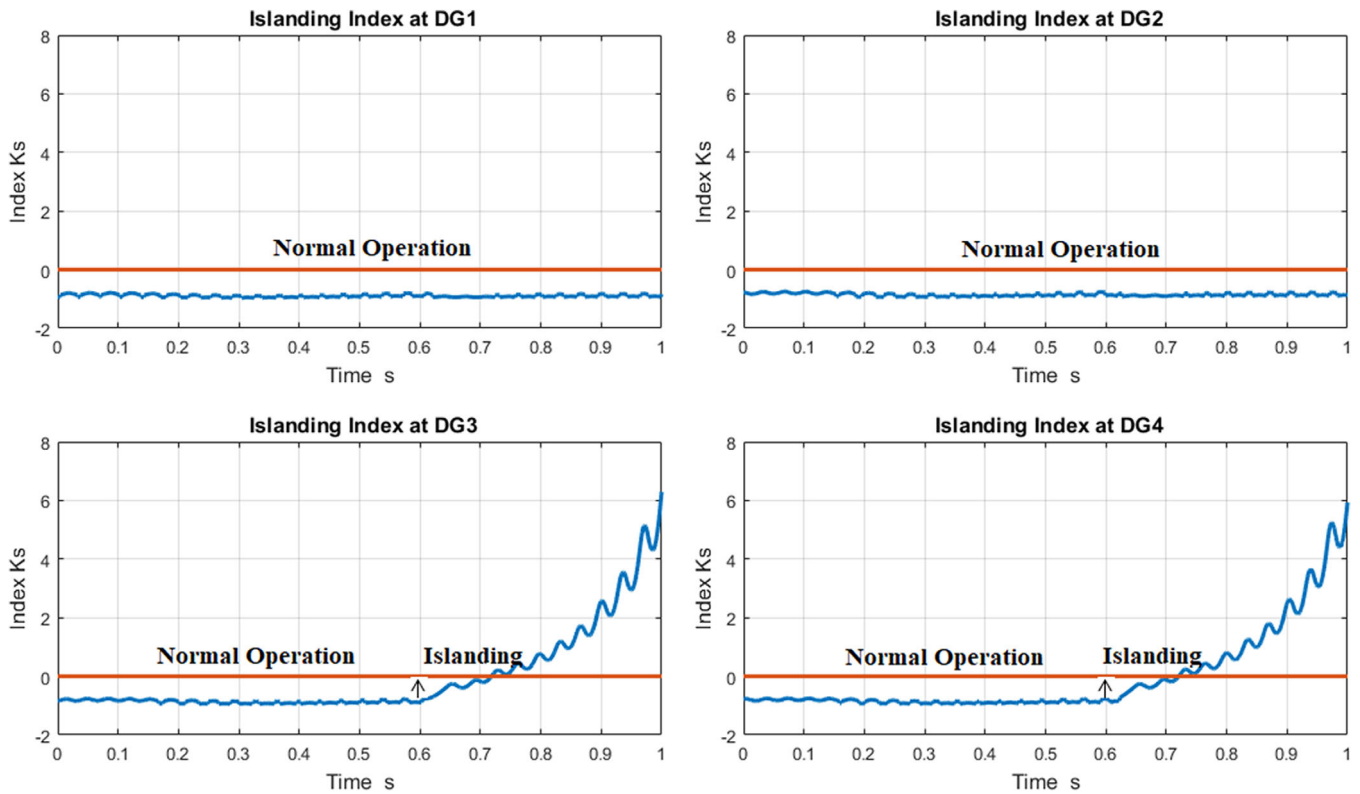


**FIGURE 13** Islanding index at DG units during the isolation of DG units (3 and 4) and the loads (L4 and L5) from the network [Colour figure can be viewed at wileyonlinelibrary.com]

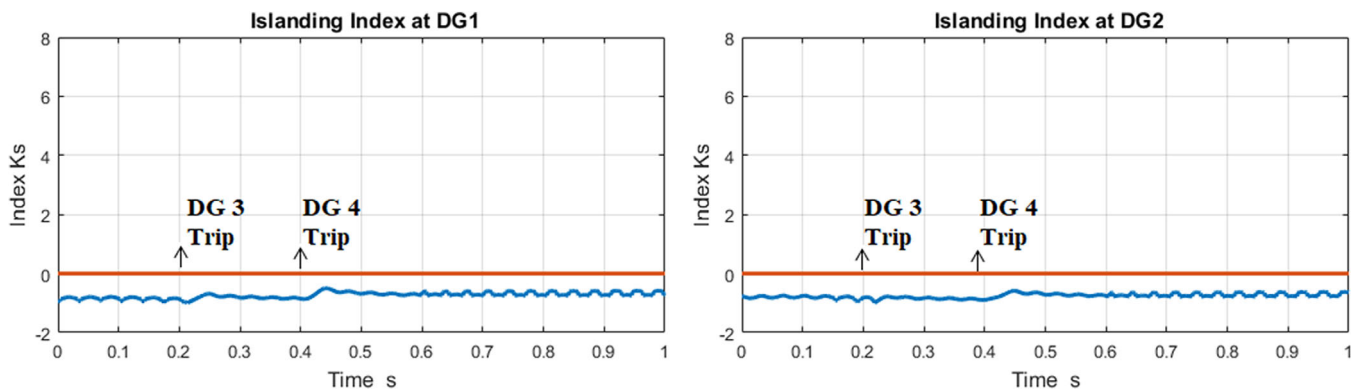


**FIGURE 14** Islanding index at DG units (1 and 2) during tripping of DG units (3 and 4) [Colour figure can be viewed at wileyonlinelibrary.com]

The simulation results of Figure 13 illustrate that once the DG units (3 and 4) are separated from the network at  $t = 0.6$  second, the islanding index at DG3 and DG4 exceeds the threshold, and the islanding index at DG1 and DG2 is below the threshold. This condition is clearly identified as islanding situation by islanding detection devices at DG3 and DG4. However, no action is done at the DG units (1 and 2) because they are outside the islanded region. The proposed method functions properly and detects islanding events under such conditions.

### 5.6 | Tripping of DG unit/DG switching events

One of the major events which may cause wrong performance in islanding detection methods is sudden DG switching events. To further investigate the proposed method performance, sudden tripping of DG unit case is simulated. This scenario is simulated by a disconnected DG unit (3) at  $t = 0.2$  second and DG unit (4) at  $t = 0.4$  second. Figure 14 indicates that once DG unit

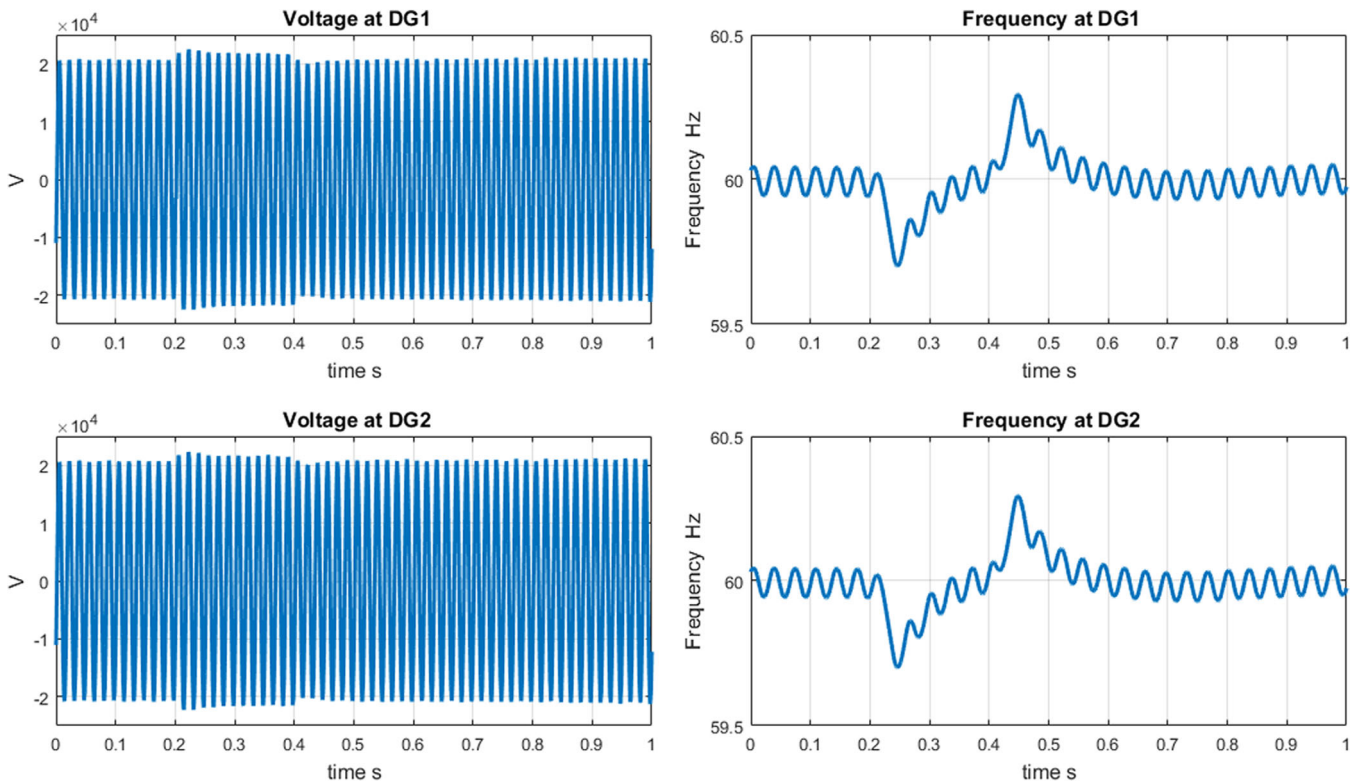


**FIGURE 15** Voltage and frequency at DG units (1 and 2) during capacitor switching [Colour figure can be viewed at [wileyonlinelibrary.com](http://wileyonlinelibrary.com)]

(3) or (4) is disconnected from the system, no remarkable variations are observed in the islanding index at other DG units (1 and 2) due to the existence of a robust grid. As a result, such tripping events have no influence on the proposed method.

## 5.7 | Capacitor switching

The response of the proposed scheme in non-islanding conditions is also tested by simulating the system under a capacitor switching. In this scenario, a capacitor of 5MVAR is switched on the network at bus DG3 at  $t = 0.2$  second and switched off at  $t = 0.4$  second when the total load demand is 20 MW and 5MVAR. During the capacitor switching, the voltage and frequency are within the allowed limits as indicated in Figure 15 and no significant changes are also detected in the islanding index as shown in Figure 16. However, remarkable changes are observed in the harmonics index at DG units as illustrated in Figure 17. Therefore, those changes initiate SRS (at  $t = 0.25$  second and  $t = 0.45$  second) at all DG units and the islanding index is observed. The simulation results of Figures 18 and 19 indicate that no changes are monitored in the islanding index at all DG units after SRS is initiated. Such switching events have no effect on the proposed strategy.

## 5.8 | Unsymmetrical faults

To further demonstrate the ability of the proposed scheme, unsymmetrical faults are proposed to study the effect of such faults on the detection of islanding condition. The proposed scheme is tested under single line to ground and double line to ground faults. The simulations are performed in such a way that the faults occur at the middle of the transmission line (at 30 km), linking DG1 and DG2, at  $t = 0.2$  second and is cleared at  $t = 0.25$  second without operation of the circuit breaker.

Simulation results shown in Figures 20 and 21 indicate that during the single line to ground fault (AG) no remarkable changes are observed in the islanding index. However, during the double line to ground fault (ABG), the islanding index exceeds the specified threshold at some DG units. Such faults may cause a malfunction for the proposed method. However, all kinds of faults are outside the scope of this paper, and they have its own protection. Therefore, to overcome such type of malfunction, a block signal is sent to form the fault protection relay to the corresponding islanding relay to ignore this case.

The logic block diagram of Figure 22 indicates this modification. The proposed method is used only to identify whether the abnormality at the point of common coupling of the DG unit is a power quality disturbance or an actual islanding operation.

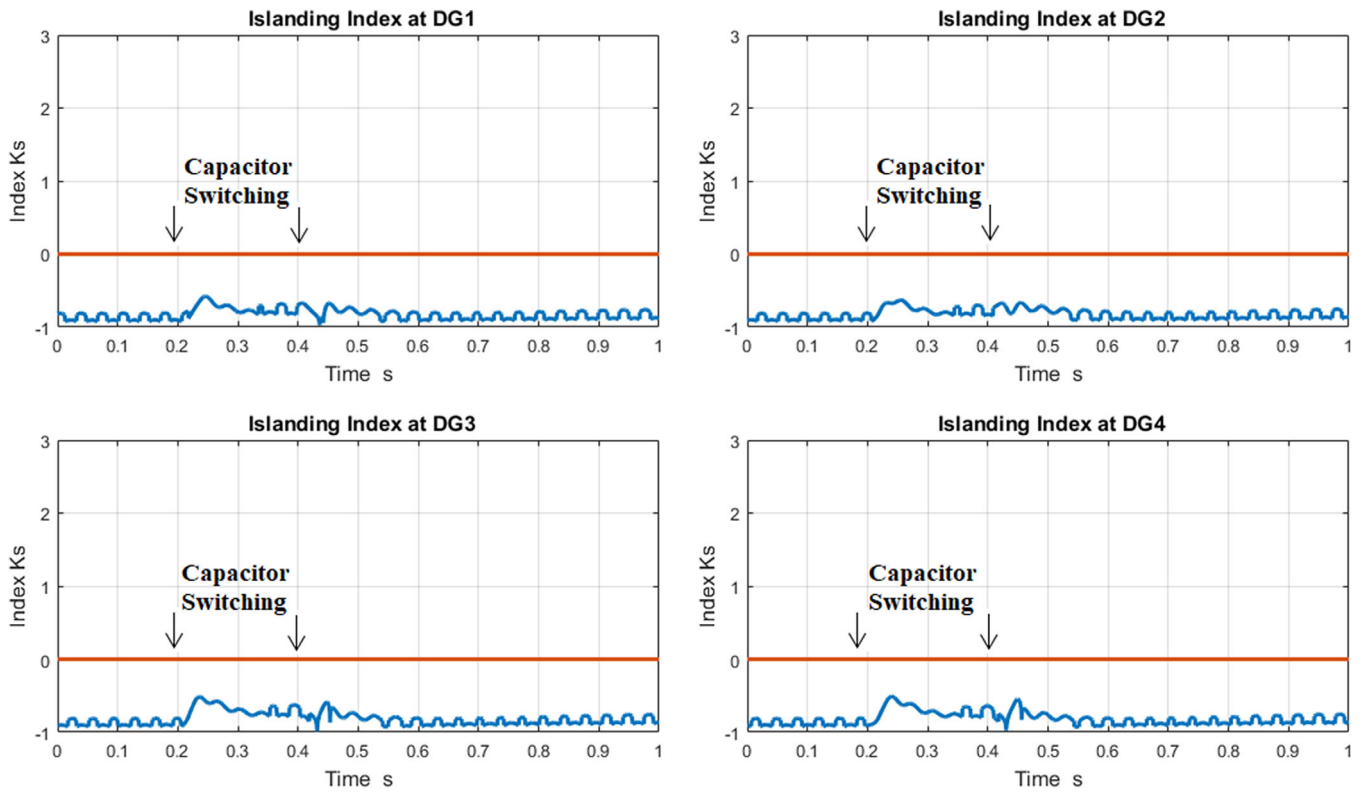


**FIGURE 16** Islanding index at DG units during capacitor switching without SRS [Colour figure can be viewed at wileyonlinelibrary.com]

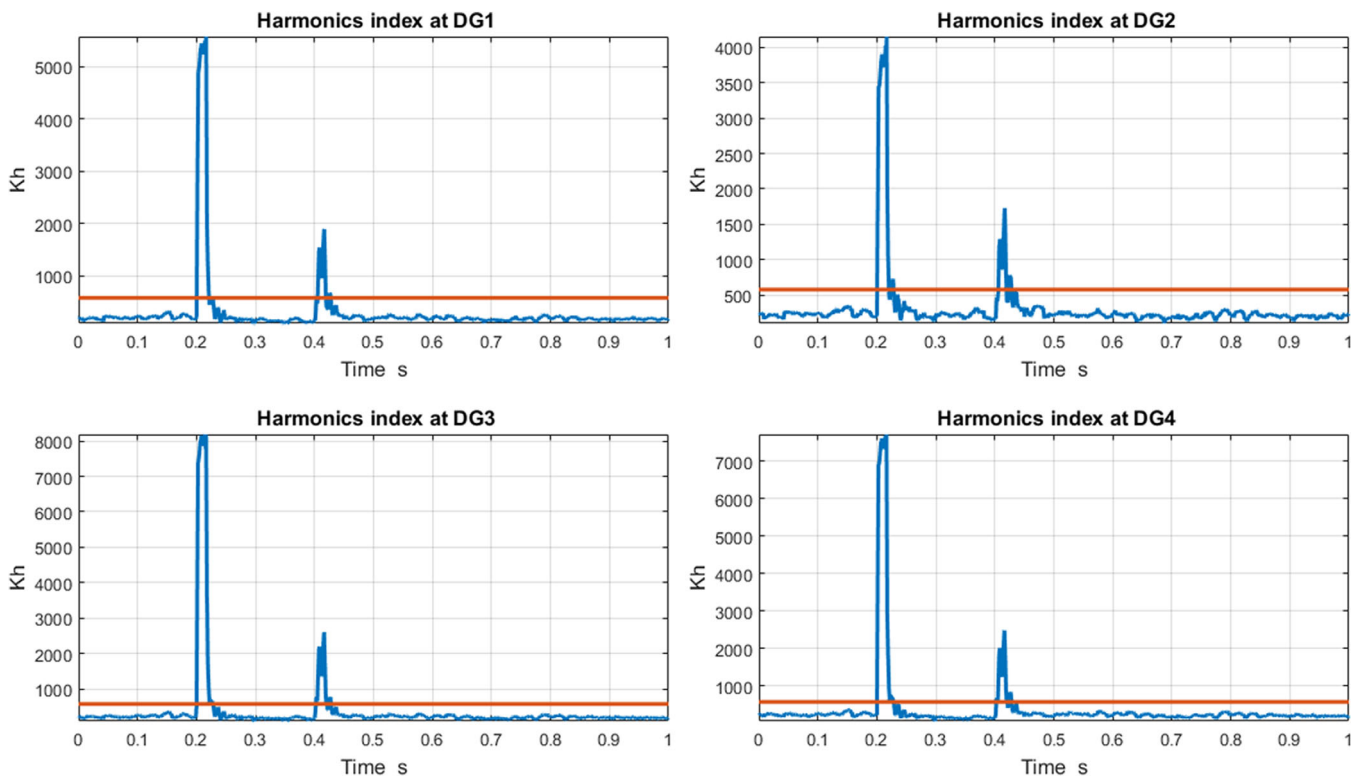


**FIGURE 17** Harmonics index at DG units during capacitor switching without SRS [Colour figure can be viewed at wileyonlinelibrary.com]

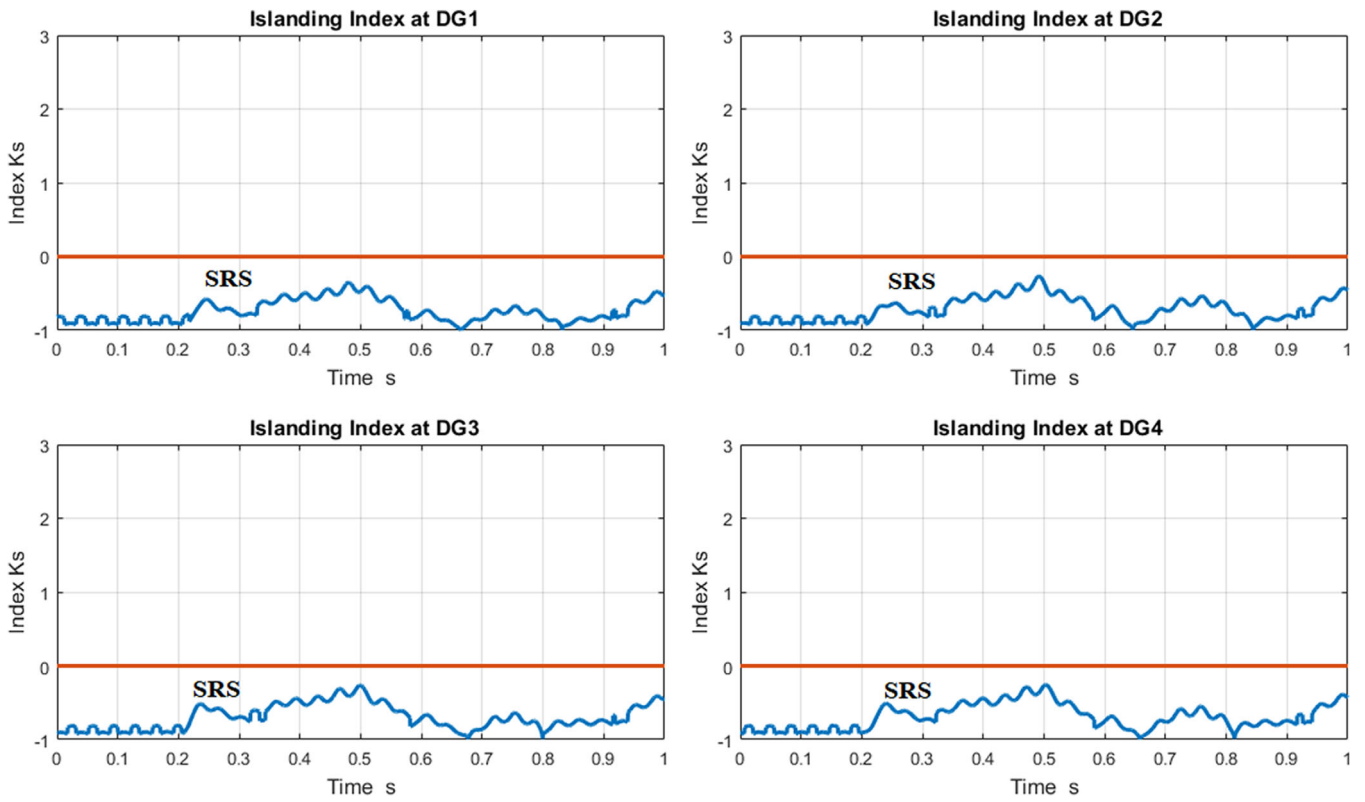


**FIGURE 18** Islanding index at DG units during capacitor switching with SRS at  $t = 0.25$  second [Colour figure can be viewed at wileyonlinelibrary.com]

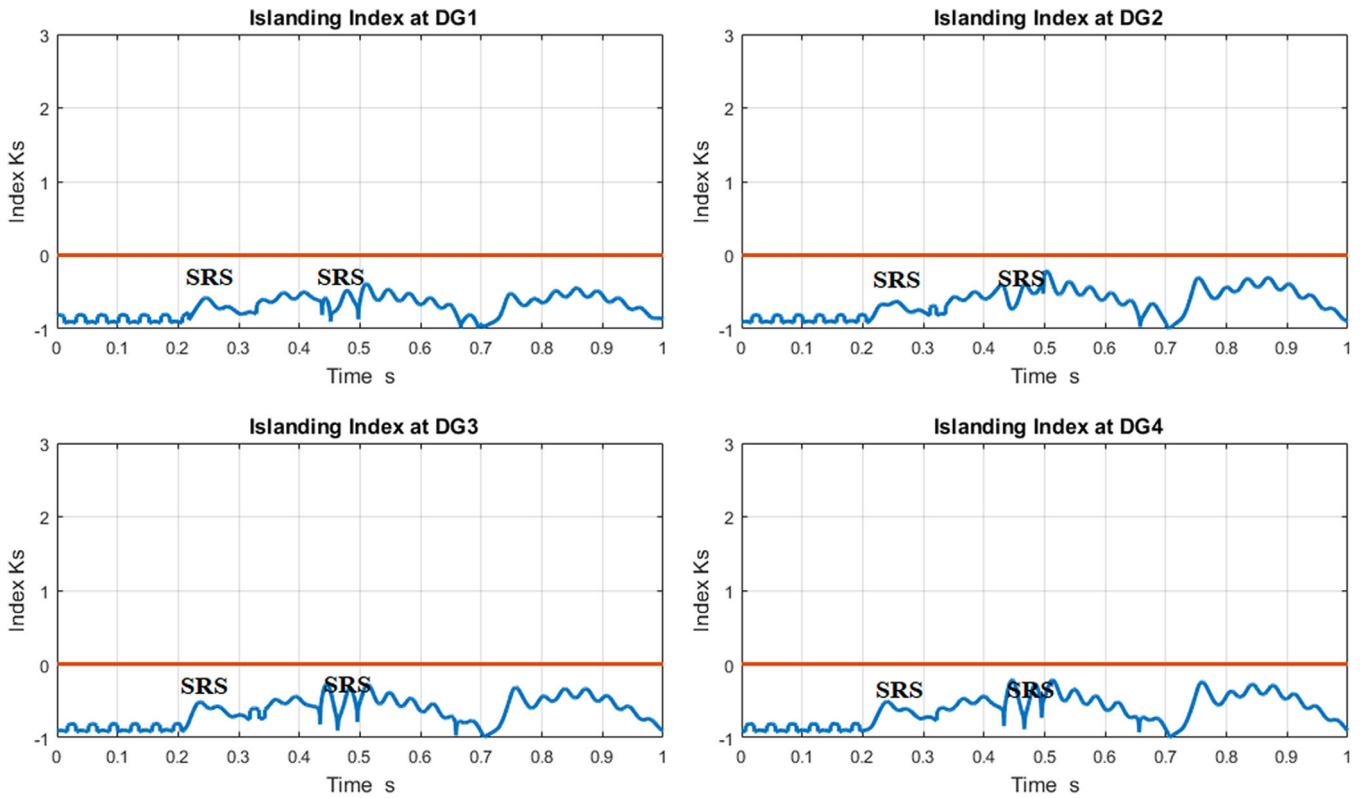


**FIGURE 19** Islanding index at DG units during capacitor switching with SRS at  $t = 0.25$  second and  $t = 0.45$  second [Colour figure can be viewed at wileyonlinelibrary.com]

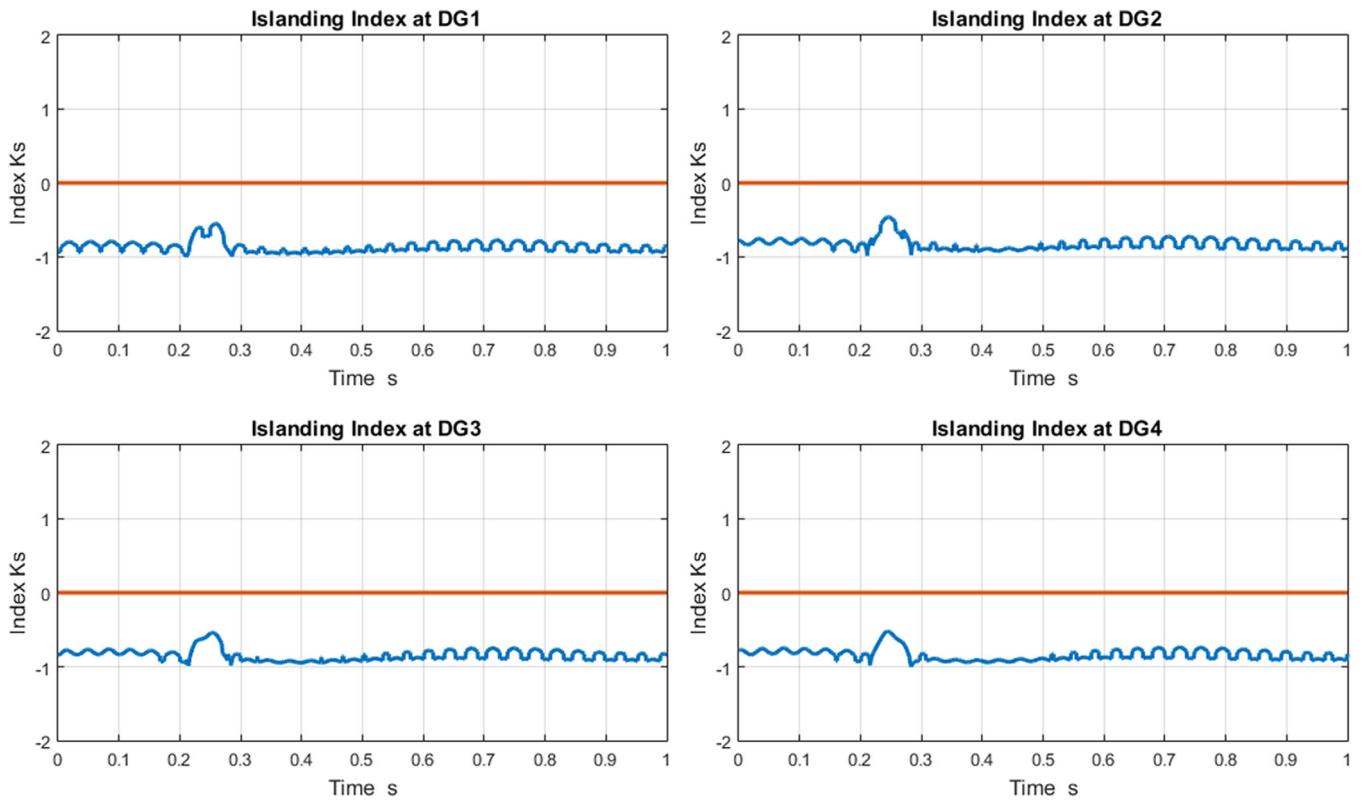


**FIGURE 20** Islanding index at DG units during single line to ground fault [Colour figure can be viewed at wileyonlinelibrary.com]

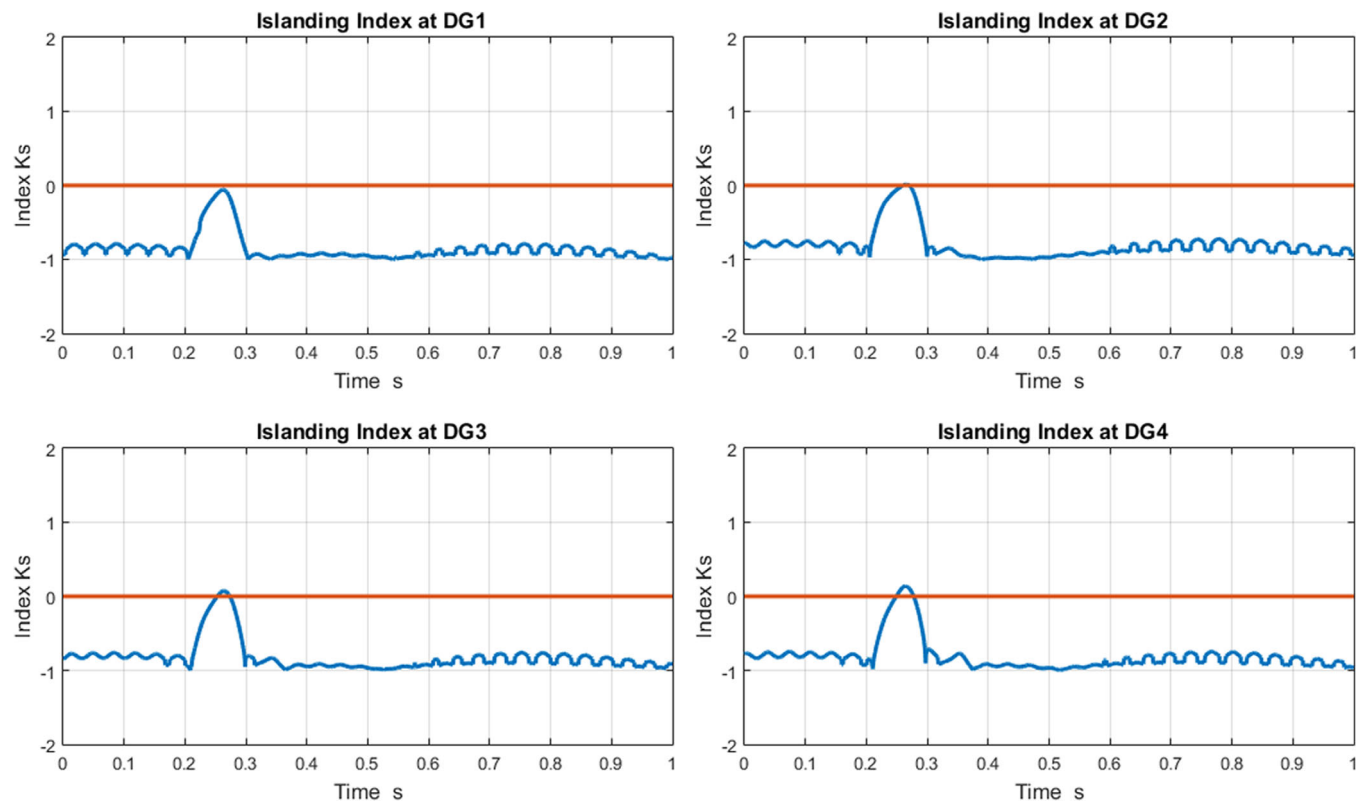


**FIGURE 21** Islanding index at DG units during double line to ground fault [Colour figure can be viewed at wileyonlinelibrary.com]

## 6 | DISCUSSION AND NDZ EVALUATION

As shown in simulation results, the proposed scheme has a desirable performance in comparison with other passive methods to detect islanding condition. During

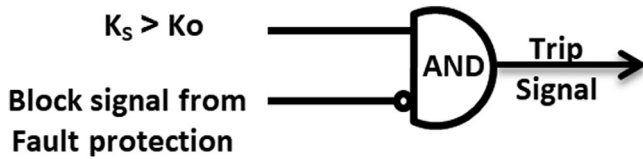


FIGURE 22 Logic diagram of the proposed method

islanding at large power mismatches, the islanding is discriminated when the islanding index is higher than zero. However, the islanding and harmonics indices are used in conjunction with the speed reduction strategy to discriminate between islanding condition at zero power mismatches and system disturbances. The performance of the proposed scheme is demonstrated through many disturbances, such as sudden load change, capacitor bank switching, DG tripping, etc. Such disturbances have no significant influence on the proposed scheme.

The proposed scheme functions properly in all cases under consideration and is capable of discriminating between islanding and non-islanding conditions, as well as it has **zero** NDZ. A summary of existing islanding schemes and their evaluation performance with respect

TABLE 3 Summary of islanding methods and their performances

Method type	Methodology	NDZ	Detection time	DG configuration	Observations
Proposed method (Passive)	Voltage and frequency variations	Zero	Small	Rotating machine based DGs	NO
Passive method <sup>20</sup>	Adaptive identifier for frequency estimation	Almost zero	Small	Synchronous and inverter based DGs	NO
Passive method <sup>19</sup>	Voltage variations	Zero	Small	All types of DGs	NO
Passive method <sup>30</sup>	Modified Slantlet transform combined with Neural network	Almost zero	Small	All types of DGs	It needs a large set of data to train and test the classifier and optimization algorithms for extracting the desirable features
Passive method <sup>15</sup>	Neural network combined with fuzzy logic.	Small	Small	All types of DGs	It needs a large set of data to train and test the classifier
Passive method <sup>31</sup>	Neural network combined with phase space algorithm.	Small	Small	Radial system with two identical DG units	It needs a large set of data to train and test the classifier
Passive method <sup>13</sup>	Voltage signal combined with neural network.	Small	Small	Single inverter system	It needs massive sample number and accuracy increases with bigger sample size
Passive method <sup>30</sup>	Slantlet transform combined with neural network	Almost zero	Small	Single inverter system	It needs a large set of data to train and test the classifier
Passive method <sup>21</sup>	Hilbert-Huang transform and learning machine	Almost zero	Small	All types of DGs	It needs a large set of data to train and test the classifier
Passive method <sup>16</sup>	Singular spectrum entropy combined with deep learning architecture.	Almost zero	Small	Single inverter system	It needs massive sample number and accuracy increases with bigger sample size
Passive method <sup>1</sup>	The dynamic behavior of load	Small	Small	All types of DGs	Threshold for islanding detection depends on the load type
Passive method <sup>33</sup>	Variational mode decomposition of voltage signals	Zero	Small	All types of DGs	Threshold value is selected based on simulation
Passive method <sup>32</sup>	Total variation filtering for a modal voltage signal	Zero	Small	Inverter based DG system	Threshold value is selected based on simulation

to methodology, NDZ, detection time, and disadvantages are indicated in Table 3.

## 7 | CONCLUSION

In this study, a new passive islanding detection strategy has been presented for rotating machine based DGs. The proposed method is based on the measurements of the system voltage and frequency to compute two indices called the islanding index and harmonics index. The islanding detection mainly depends on the islanding index. The harmonics index and speed reduction strategy are used to assist discrimination between islanding condition at a close power mismatch and system disturbances. Many system disturbances are simulated to show the performance and effectiveness of the proposed scheme under all conditions.

The results of the simulation indicate that the proposed strategy functions correctly in islanding and non-islanding conditions. Furthermore, unlike many detection methods, a simple computational procedure has been presented to calculate the threshold for islanding detection. This threshold is important so that it avoids the non-detection zone. Moreover, the proposed scheme has “zero” NDZ, as demonstrated in the simulations, and can be applied for rotating machine-based DG units. During the simulation, the maximum detection time of the islanding situation is about 350 ms. Finally, the scheme is simple, easy to implement in practice, and has no effect on the power quality or the stability of the network.

## REFERENCES

- Xing Xie, Chun Huang\*, Danni Li. A new passive islanding detection approach considering the dynamic behavior of load in microgrid. *Electr Power Energy Syst* 2020; 117: 105619.
- Papadimitriou CN, Kleftakis VA, Hatziaargyriou ND. A novel islanding detection method for microgrids based on variable impedance insertion. *Electr Pow Syst Res*. 2015;121:58-66.
- Shrivastava S, Jain S, Nema RK, Chaurasia V. Two level islanding detection method for distributed generators in distribution networks. *Electr Power Energy Syst*. 2017;87:222-231.
- Li C, Cao C, Cao Y, Kuang Y, Zeng L, Fang B. A review of islanding detection methods for microgrid. *Renew Sustain Energy Rev*. 2014;35:211-220.
- X1OstojićMM, Djurić MB. The algorithm with synchronized voltage inputs for islanding detection of synchronous generators. *Electr Power Energy Syst*. 2018;108:431-439.
- Khamis A, Shareef H, Bizkevelci E, Khatib T. A review of islanding detection techniques for renewable distributed generation systems. *Renew Sustain Energy Rev*. 2013;28:483-493.
- Ku Ahmad KNE, Selvaraj J, Rahim NA. A review of the islanding detection methods in grid-connected PV inverters. *Renew Sustain Energy Rev*. 2013;21:756-766.
- Guo X, Xu D, Wu B. Overview of anti-islanding US patents for grid-connected inverters. *Renew Sustain Energy Rev*. 2014;40: 311-317.
- Motter D, Vieira JCM. Improving the islanding detection performance of passive protection by using the undervoltage block function. *Electr Pow Syst Res*. 2020;184(1-10):106293.
- IEEE Guide for Design. Operation and integration of distributed resource Island systems with electric power systems. *IEEE Standards*. 2011;1547:4-2011.
- Abd-Elkader et al. Islanding detection method for DFIG wind turbines using artificial neural networks. *Electr Power Energy Syst*. 2014;62:335-343.
- Ahmadipour M, Hizam H, Othman ML, Radzi MAM, Murthy AS. Islanding detection technique using Slantlet transform and Ridgelet probabilistic neural network in grid-connected photovoltaic system. *Appl Energy*. 2018;231:645-659.
- Merlin VL, Santos RC, Grilo AP, Vieira JCM, Coury DV, Oleskovicz M. A new artificial neural network based method for islanding detection of distributed generators. *Electr Power Energy Syst*. 2016;75:139-151.
- Isazadeh G, Kordi M, Eghtedarnia F, Torkezadeh R. A new wide area intelligent multi-agent islanding detection method for implementation in designed WAMPAC structure. *Energy Procedia*. 2017;141:443-453.
- Shayeghi H, Sobhani B, Shahryari E, Akbarimajd A. Optimal neuro-fuzzy based islanding detection method for distributed generation. *Neurocomputing*. 2016;177:478-488.
- Kong X, Xu X, Yan Z, Chen S, Yang H, Han D. Deep learning hybrid method for islanding detection in distributed generation. *Appl Energy*. 2018;210:776-785.
- Pinto SJ, Panda G. Performance evaluation of WPT based islanding detection for grid-connected PV systems. *Electr Power Energy Syst*. 2016;78:537-546.
- Samantaray SR, el-Arroudi K, Joos G, Kamwa I. A fuzzy rule based approach for islanding detection in distributed generation. *IEEE Trans Power Deliv*. 2010;25(3):1427-1433.
- Abd-Elkader AG, Saleh SM, Magdi Eiteba MB. A passive islanding detection strategy for multi-distributed generations. *Electr Power Energy Syst*. 2018;99:146-155.
- Bakhshi M, Noroozian R, Gharehpetian GB. Islanding detection scheme based on adaptive identifier signal estimation method. *ISA Trans*. 2017;71:328-340.
- Mishra M, Sahani M, Rout PK. An islanding detection algorithm for distributed generation based on Hilbert-Huang transform and extreme learning machine. *Sustain Energy Grids Netw*. 2017;9:13-26.
- Sirjani R, Okwose CF. Combining two techniques to develop a novel islanding detection method for distributed generation units. *Measurement*. 2016;81:66-79.
- Zamani R et al. Islanding detection of synchronous machine-based distributed generators using signal trajectory pattern recognition. *6th International Istanbul Smart Grids and Cities Congress and Fair*. Istanbul, Turkey: IEEE; 2018.
- Gupta P, Bhatia RS, Jain DK. Average absolute frequency deviation value based active islanding detection technique. *IEEE Trans Smart Grid*. 2015;6(1):26-35.
- Alshareef S, Talwar S, Morsi WG. A new approach based on wavelet design and machine learning for islanding detection of distributed generation. *IEEE Trans Smart Grid*. 2014;5(4):1575-1583.

26. Do HT et al. Passive-islanding detection method using the wavelet packet transform in grid-connected photovoltaic systems. *IEEE Trans Power Electron.* 2016;31(10):6955-6967.
27. Ahmadipour M, Hizam H, Lutfi Othman M, Amran Mohd Radzi M. An anti-islanding protection technique using a wavelet packet transform and a probabilistic neural network. *Energies.* 2018;11(10):2701.
28. Shayeghi H, Sobhani B. Zero NDZ assessment for anti-islanding protection using wavelet analysis and neuro-fuzzy system in inverter based distributed generation. *Energ Convers Manage.* 2014;79:616-625.
29. Mlakić D et al. A novel ANFIS-based islanding detection for inverter-interfaced microgrids. *IEEE Trans Smart Grid.* 10(4):2018.
30. Ahmadipour M, Hizam H, Lutfi Othman M, Radzi MAM, Chireh N. A novel islanding detection technique using modified Slantlet transform in multi-distributed generation. *Electr Power Energy Syst.* 2019;112:460-475.
31. Khamis A, Shareef H, Mohamed A, Bizkevelci E. Islanding detection in a distributed generation integrated power system using phase space technique and probabilistic neural network. *Neurocomputing.* 2015;148:587-599.
32. Mishra PP, Bhende CN, Manikandan MS. Islanding detection using total variation-based signal decomposition technique. *IET Energy Syst Integr.* 2020;2:22-31.
33. Admasie S, Bukhari SBA, Haider R, Gush T, Kim C-H. A passive islanding detection scheme using variational mode decomposition-based mode singular entropy for integrated microgrids. *Electr Pow Syst Res.* 2019;177:105983.

**How to cite this article:** Abd-Elkader AG, Saleh SM. Zero non-detection zone assessment for anti-islanding protection in rotating machines based distributed generation system. *Int J Energy Res.* 2020;1–20. <https://doi.org/10.1002/er.5705>